ICING TUNNEL TESTS OF A GLYCOL-EXUDING POROUS LEADING EDGE ICE PROTECTION SYSTEM ON A GENERAL AVIATION AIRFOIL

KU-FRL-464-1

Prepared by

David L. Kohlman, William G. Schweikhard, and Alan Albright
University of Kansas
Lawrence, Kansas
and
Peggy Evanich
NASA Lewis Research Center
Cleveland, Ohio

for

Lewis Research Center
National Aeronautics and Space Administration
under NASA Grant NAG 3-71

Flight Research Laboratory
University of Kansas Center for Research, Inc.
Lawrence, Kansas 66045

May 1981

SUMMARY

A glycol-exuding porous leading edge ice protection system was tested in the NASA Icing Research Tunnel at Lewis Research Center. Test results showed that the system was very effective in preventing ice accretion (anti-ice mode) or removing ice from an airfoil. Minimum glycol flow rates required for anti-icing are a function of velocity, liquid water content in the air, ambient temperature, and droplet size. Large ice caps were removed in only a few minutes using anti-ice flow rates, with the shed time being a function of the type of ice, size of the ice cap, angle of attack, and glycol flow rate. Wake survey measurements showed that no significant drag penalty was associated with the installation or operation of the system tested.

INTRODUCTION

At the present time the only ice protection system available in the U.S. for light airplane wings is a pneumatic boot system. While this concept has been relatively successful, there are some disadvantages. The boots are expensive and must be replaced periodically. The boots do not prevent ice but remove it after it has formed. This causes two problems: some ice may remain adhered to the boot; and premature actuation of the boot may only displace--not remove--the ice, making further removal difficult. Pilot judgement is therefore a factor that influences the performance of the system. Furthermore, any ice that forms on the wing aft of the active portion of the boot will not be removed. This may be substantial, especially at high angles of attack. Recently, considerable difficulty has been experienced in finding a boot configuration that will be effective on airfoils with large leading edge radii, a feature

which characterizes several new low speed airfoils developed by NASA.

One alternative to the pneumatic boot is a liquid ice protection system that distributes a glycol solution onto the leading edge of a wing or control surface through a porous skin. This concept was developed by T.K.S. (Aircraft De-Icing) Ltd, of England, and subsequently employed on numerous airplanes.

There are several advantages associated with a porous leading edge ice protection system:

- Leading edge airfoil contours can be retained with excellent tolerance.
- No residual or runback ice is left on surfaces after system actuation.
- The life of the system hardware is comparable to that of the airframe.
- The system operates with a low power demand.
- Little judgement is required by the pilot to operate the system safely.

A disadvantage is that the glycol solution must be carried on board whenever the need for ice protection is anticipated. Furthermore, the duration of ice protection is limited by the finite supply of fluid. Obviously, it is desirable to establish the minimum fluid flow rates required to obtain the level of protection desired.

Little is known about porous leading edge ice protection systems in the United States, and no American-built airplanes employ such a system as factory-installed equipment. Thus there is a need to increase understanding of this option and to generate a data base for designers to use in the future.

The purpose of these tests is to determine the operating characteristics of a porous leading edge glycol system on an advanced low speed airfoil and to define minimum effective glycol flow rates at various flight conditions.

SYMBOLS

C_d	section drag coefficient, $2\int V_1/V(1 - V_1/V)dx$
C_ℓ	section lift coefficient
H	local stagnation pressure
H_o	free stream stagnation pressure
LWC	liquid water content, gm/m^3
p_o	free stream static pressure
T	total temperature
V	free stream equivalent airspeed
V_1	local equivalent airspeed
WS	wing station, in
x,y	position coordinates
α	angle of attack

TUNNEL DESCRIPTION AND TEST CONDITIONS

The NASA Lewis Icing Research Tunnel (IRT) is a closed cycle refigerated wind tunnel with a rectangular test section 1.83 m (6 ft.) high by 2.74 m (9 ft.) wide by 6.1 m (20 ft.) long (Figure 1). Maximum tunnel airspeed is 134 m/sec (300 mph). A natural icing cloud is simulated by injecting a water spray upstream of the test section.

The area of interest on the test model is confined to that region in the center of the test section where the icing cloud is most uniform, covering a cross-sectional area of .9 m (3 ft.) high by 1.5 m (5 ft.) wide. The liquid

water content (LWC) of the cloud can be varied from about .5 to over 2 g/m^3 with volume median droplet diameters in the range of 10 to 20 microns. The tunnel airflow temperature can be varied from -28.9°C (-20°F) to ambient.

For this series of tests two test section equivalent airspeeds were chosen, namely 49.2 m/sec (96 knots) and 90.3 m/sec (175 knots). These speeds correspond to the best rate of climb speed and the cruise speed of an aircraft on which a NACA 64 series airfoil is typically used.

Since the LWC and water drop size ranges of the IRT icing cloud depended upon tunnel airspeed, operating envelopes for LWC and drop size were plotted for the given airspeeds of interest, 49.2 m/sec and 90.3 m/sec (Figure 2). From these two tunnel operating envelopes the extreme values and several mid-point values of LWC and drop size were chosen as the icing cloud test conditions (Figure 2). The LWC and drop size varied then from .65 to 2.4 g/m^3 and 11 to 20 microns, respectively. Figures 3 and 4 illustrate where the tunnel icing cloud test conditions are located on the continuous maximum and intermittent maximum icing condition curves specified in FAR Part 25 (ref. 1).

The type of ice (i.e., glaze or rime) that formed on the airfoil depended primarily on the tunnel total air temperature. To produce glaze ice the tunnel total air temperature was set at -3.9°C (25°F), and to produce rime ice it was set at -15°C (5°F). The ambient or outside air temperature (OAT) corresponds to the static air temperature in the tunnel test section. For the two airspeeds chosen, namely 49.2 m/sec and 90.3 m/sec, the OAT's for glaze ice were -5.1°C and -7.8°C, respectively; and the OAT's for rime ice were -16.2°C and -18°C, respectively. The true airspeeds were 43.7 m/sec and 85.3 m/sec at T = 5°F and 44.7 m/sec and 86.9 m/sec at T = 25°F.

A translating wake-survey probe was used to measure the section drag coefficient, C_d, of the test model. The probe consisted of a single stagnation pressure tube which could be retracted behind a wind screen. When the airfoil was exposed to the tunnel icing cloud, the probe was retracted. After the icing cloud was turned off, the probe was inserted into the airstream and the wake survey was made. This probe, which was located about one chord length downstream of the airfoil at midspan, was installed as shown in Figure 5 to yield the velocity decrement ratio (V_1/V) in the airfoil wake. By translating laterally through the wake, a plot of V_1/V versus position was obtained. Integration of the wake defect gave a measurement of model section drag coefficient.

MODEL DESCRIPTION

The wing section tested was taken from an actual single engine light airplane. The original wing tapered from a NACA 64_2A215 airfoil at the root (WS 0) to a NACA 64_1A412 airfoil at the tip (WS 216). The wing incorporated a modification proposed by Raymond Hicks (refs. 2, 3) of NASA Ames Research Center. This modification, which adds thickness to the forward 30 percent of the upper surface, increases $C_{\ell_{max}}$, reduces C_d at high C_ℓ, and improves stall characteristics. A typical "Hicks" modification is shown in Figure 6.

The wing section tested was fastened securely to the turntable on the floor of the tunnel, using the spar fittings that are used to attach the wing to the fuselage of the airplane. A clearance of one-half inch was allowed between the outboard end of the wing segment and the ceiling of the six-foot high test section of the tunnel. The centerline of the tunnel was at WS 58

of the original wing. Table 1 gives the airfoil coordinates at WS 58, where the wing chord is 63.25 inches. The chord tapers 1.1 inches per foot of span, and the wing is twisted 0.167 degrees per foot of span (washout). Figure 7 shows the wing section installed in the NASA Lewis Icing Research Tunnel.

ICE PROTECTION SYSTEM DESCRIPTION

The system tested consists of porous stainless steel panels attached to the leading edge of the wing, and a pump that distributes a glycol based fluid from a tank to the panels through plastic tubing. The fluid exudes from the porous panels onto the surface of the wing, providing either an anti-icing capability by dissolving the supercooled water droplets and preventing the formation of ice, or a deicing capability by chemically breaking the bond of established ice. A significant feature of the system is that protection is obtained aft of the panels by the flow of the fluid along the chord to the trailing edge, thus preventing the formation of ice anywhere aft of the active leading edge.

The porous leading edge panel used in this test was attached to the original wing leading edge, as shown in the cross-sectional drawing in Figure 8. The width of the porous region is 8.7 cm. The panel is divided spanwise into three separate porous sections. Referring to the vertical position of the wing in the tunnel, the upper and lower sections are 20.3 cm long and the middle section is 30.4 cm long. The maximum thickness of the T.K.S. panel is 3.2 mm. The flow rate into each section was controlled independently by three variable positive displacement pumps.

The fluid reservoir behind the porous leading edge skin consists of a solid stainless steel backing plate and a thin polyvinylchloride sheet that separates the fluid from the porous leading edge. The purpose of the polyvinylchloride sheet, whose porosity is much lower than that of the stainless steel, is to distribute the glycol evenly over the entire active portion of the panel, regardless of the chordwise pressure distribution changes that occur as angle of attack changes.

The porous stainless steel skin consists of two layers of wire cloth that are rolled, sintered, and then finish-rolled to thickness. The wire cloth is manufactured from an 18-8 austenitic stainless steel and nominally has 110 x 20 wires per inch. The two layers are oriented 90° with respect to each other. Figure 9 shows a portion of the porous panel installed on the test wing section. The system hardware was designed and manufactured by T.K.S. (Aircraft De-Icing) Ltd.

The fluid used in this test is composed of 80% mono-ethylene glycol and 20% de-ionized water.

The edges of the active portion of the panel must be placed such that extreme positions of the stagnation points for which icing protection is required are no closer to the edge than approximately 1 cm. This ensures that the fluid will always be distributed on both the upper and lower surface of the wing. Figure 8 shows the location of the stagnation points on the leading edge for each angle of attack used in this test.

TEST RESULTS

Table 2 contains a summary of all the runs made and the primary data for each run. Note that the run numbers are not consecutive because the run numbers and conditions were established prior to testing, and time constraints forced the elimination of some runs. The sections that follow present data in graphical form and discuss in detail the results for each of the three modes in which the system was tested.

Anti-ice Mode

Normal operation of the glycol-exuding porous leading edge system is in the anti-ice mode; that is, the glycol flow rate is sufficient to prevent any ice from forming on the wing. This is possible as long as the glycol-water solution on the surface maintains a freezing temperature below the ambient air temperature. The solution freezing temperature increases as the ratio of the water catch rate to the glycol flow rate increases. A series of runs was conducted in the Lewis IRT to determine the minimum glycol flow rate at which anti-icing could be maintained.

The method of determining the glycol flow rate corresponding with the anti-ice threshold was as follows. At a given flight condition, the flow rate was set to be well above the anti-ice threshold. The flow rate was then reduced in steps, allowing about 30 seconds for the system to stabilize at each point, until small flecks of ice began to appear on the leading edge in the vicinity of the stagnation point. At the anti-ice threshold, the small ice flecks, ranging up to about 3 mm in diameter, would form and then be swept downstream in only a few seconds. A glycol flow rate lower than the threshold

value would cause the ice flecks to persist, gradually growing into larger patches before being shed from the wing.

To obtain the minimum anti-ice glycol flow rates, the upper and lower sections were used simultaneously during each run to establish independent flow rate values from each section while the center section was used to determine minimum flow rates for natural deicing (discussed in the next section). The data presented represent an average of the results from the upper and lower sections. As a general rule, the anti-ice threshold occurred at a lower flow rate on the lower section than on the upper section. This can be attributed to the larger leading edge radius of the lower section, which results in a reduced water catch rate at the leading edge. The average should closely represent the anti-ice threshold on the center section. Flow rates are presented in terms of specific fluid flow: milliliters of glycol per square centimeter of active panel per minute.

Figures 10a through 10d present the results of anti-ice tests at the two airspeeds and temperatures used for this study. Specific fluid flow is shown as a function of angle of attack for several liquid water contents at each flight condition. Minimum anti-ice fluid flows are not strongly affected by angle of attack, as long as the stagnation point is not too close to the edge of the porous skin. As seen in Figure 8, the stagnation point for $\alpha = -.5°$ is closest to the edge. This angle of attack tends to require a higher flow rate, particularly at the higher airspeed. For $\alpha = 12°$, the stagnation point is not as close to the edge as for $\alpha = -.5°$, and the effect of the edge is not evident in the data.

As one would expect, required glycol flow rates generally increase as LWC increases and as airspeed increases. However, the width of the threshold

in terms of glycol flow rate, the subjective task of identifying the threshold, and the normal variations in LWC during a series of runs resulted in a sometimes broad band of uncertainty in the data as shown in Figure 10c.

One method to check for consistency in anti-ice threshold data is to plot glycol flow as a function of LWC, all other conditions being constant. To first order accuracy, the result should be a straight line through the origin with positive slope, since an increase in water collection at the leading edge should require a proportionate increase in glycol to maintain a solution at the threshold of freezing.

Figures 11a through 11d illustrate results for the anti-icing tests. In general, the fluid flow rates do increase monotonically as LWC increases, frequently approximating the straight line through the origin that would be expected. Obvious variances do appear, however, and illustrate test points that probably were not run long enough to determine the flow rate at the lower end of the threshold. In virtually every case, the variance in flow rate appears to be higher than the expected value.

One other point needs to be made. One variable that does not appear explicitly in Figures 11a through 11d is the water droplet diameter. As the droplet size increases, the catch rate of the wing will increase also because of the higher inertia of each drop. This will require a higher glycol flow rate to maintain anti-icing at the same LWC. However, the data do not indicate that this effect is much greater than the uncertainty in the data, over the range of 11 to 20 microns used in these tests.

A designer might well be concerned whether these flow rates would be adequate to meet certification requirements. As shown in Figures 3 and 4, the maximum droplet size specified by FAR Part 25 is 30 microns; and as droplet

size increases from 20 to 30 μm, the LWC decreases significantly. Further studies are now in progress to define more accurately the effect of droplet size on flow rate required and to develop a reasonably accurate analytical method of predicting minimum anti-ice glycol flow rates.

Natural Deice Mode

The natural deice mode occurred when the glycol flow rate was below the anti-ice threshold value, but still high enough that no permanent ice accretions formed on the wing. It was subjectively identified by the formation of a continuous spanwise bar of ice along the stagnation line, about 3 to 7 mm thick and 5 to 10 mm wide, which would shed at intervals of approximately 2 to 7 minutes. The threshold was identified as the lowest specific fluid flow at which periodic shedding of the bar of ice would take place.

Results are presented in Figures 12a through 12d. Again, the required glycol flow rates are not a strong function of angle of attack except at 175 knots and 5°F, where the flow rates increase significantly as the stagnation point approaches either edge of the porous panel. The band of uncertainty is observed to be near the variation caused by the difference in LWC.

The natural deice flow rates were substantially lower than those for anti-icing, often being as low as 25% to 50% of the anti-ice threshold. This implies that a system designed for anti-icing at a given LWC can safely withstand much more severe icing conditions, operating in the natural deicing mode.

Deicing Tests

It is possible that a pilot might fly in icing conditions for a period of time before becoming aware of the situation, particularly at night. Therefore it is of interest to determine the capability of the porous leading edge system to shed ice after an initial buildup with the flow pump turned off.

The test procedure was as follows. The center section glycol was turned off, and the upper and lower sections were provided a flow rate equal to or greater than the minimum required for anti-icing. This prevented the ends of the ice cap from adhering to an untreated portion of the leading edge, thus influencing the results. At each test condition the icing spray was turned on for a specific period of time. After the spray was turned off, the center section glycol pump was turned on at a given rate and the time required to shed completely the cap of ice from the leading edge was determined.

Results of the deicing tests are presented in Figures 13 and 14. General observations are that the higher the glycol flow rate the shorter the time required to shed the ice (although very high flow rates bring diminishing returns), and reasonable ice shedding times can be achieved with glycol flow rates that are comparable to flow rates required for operation in the anti-ice mode.

Figure 13 shows that the deicing time is dependent on angle of attack. With $\alpha = 7.8°$, the deicing time may be as low as one-half that for $\alpha = 1.2°$. Extreme angles, where the stagnation point approaches the edge of the active panel, should be avoided.

An interesting phenomenon may be observed in Figure 14. For a temperature of 25°F, the longer the ice is permitted to build up, the longer it takes to

remove it--a result that might have been expected. However, at 5°F a larger ice cap is shed more quickly than a smaller ice cap at the same specific fluid flow.

The explanation is that at 25°F glaze ice is formed, which is accompanied by runback icing and a wide ice cap. As the icing exposure time increases, the ice cap becomes more firmly attached to the leading edge, particularly at the edges of the porous skin. Therefore, as the icing time increases, so does the time required for the glycol to completely break the bond between the ice and the wing skin.

At 5°F, only rime ice forms. This ice freezes almost immediately on contact with the wing; thus, the ice cap tends to remain concentrated near the stagnation point on the porous panel. In this case, the time required to shed the ice depends strongly on the aerodynamic forces acting on the ice. Since these forces are roughly proportional to the size of the cap, the larger caps tend to shed more quickly, at least for the icing durations used in these tests.

In several cases it was observed that a small change in angle of attack would precipitate the shedding of an ice cap because of the increased aerodynamic force on the ice caused by the altered flow field.

Figure 15 is a sequence of photographs showing the progressive shedding of an ice cap formed at T = 25°F, V = 96 knots, α = 7.8°, and liquid water content LWC = 2.40 gm/m^3. The droplet mean size was 20 microns. Icing spray time was 10 minutes. The glycol specific fluid flow was 0.052 ml/cm^2/min. The bottom surface of the wing is shown. Note that by the time the leading edge ice is shed, the runback of glycol along the wing surface has substantially removed the frost and ice particles well behind the active portion of the leading edge.

Drag Measurements

The wake survey probe described previously was used to measure the effect of the porous panel, various modes of operation, and different amounts of ice on the section drag coefficient of the wing. The results are shown in Figure 16.

The porous panel adds less than .001 to the section drag of the wing, within the uncertainty band of the drag measuring system. The penalty of carrying ice is clearly seen in the 50% to 100% increase in C_d, depending on angle of attack, caused by a 10 minute accumulation of ice.

After deicing, the drag is almost back to the clean level, except for the effect of some residual frost and ice particles on the lower surface of the wing. The anti-ice mode has practically no effect on the section drag.

DISCUSSION AND CONCLUSIONS

The data obtained in these tests provide useful information on the glycol flow rates required to obtain satisfactory ice protection performance from a porous leading edge system. Although the data apply to only the airfoil tested, the range represented should be typical for most light airplane wings.

In most cases satisfactory performance can be obtained with much lower flow rates. As shown in Figure 3, the extreme conditions tested represent a LWC three times higher than the upper boundary of the continuous maximum conditions defined by FAR Part 25. The upper boundary of the intermittent maximum conditions is just met. The results showed that extremely severe conditions can be handled by a liquid protection system if the condition is only temporary.

The system merely reverts to the natural deicing or deicing mode until conditions permit a return to the anti-ice mode. It would be possible to operate the system at two different flow rates.

It would be desirable to be able to predict accurately the minimum flow rates required to achieve anti-icing at various flight conditions. Reference 4 provides an empirical method, but investigation showed that this method was limited in range and required assumptions that limited the accuracy of the prediction for this airfoil. In a follow-on study, methods are being developed to obtain reasonably accurate predictions of minimum flow rates, so that design evaluations of various configurations can be made without the necessity for icing tunnel tests.

Additional icing tunnel testing is also planned so that more data can be obtained for purposes of comparison, questionable data points can be resolved, and the effect of droplet diameter can be assessed.

As a result of the tests reported herein, the following conclusions have been made:

1. A glycol-exuding porous leading edge ice protection system is a very effective means of preventing ice accretion or removing ice from an airfoil.
2. The stagnation point may come within one centimeter of the edge of the porous surface without seriously degrading the performance of the system.
3. The system tested was able to remove large ice caps with glycol flow rates normally used in the anti-ice mode.
4. The type of ice formed and the angle of attack have a significant effect on the deicing time.

5. No significant drag penalty was associated with the installation or operation of the system tested.

REFERENCES

1. Federal Aviation Regulations, Part 25, Appendix C - Airworthiness Standards: Transport Category Airplanes. Department of Transportaion, Federal Aviation Administration, Washington, D.C., June 1974.

2. Hicks, R. M., and Schairer, E. T., "Effects of Upper Surface Modification on the Aerodynamic Characteristics of the NACA 63_2-215 Airfoil Section." NASA TM 78503, January 1979.

3. Szelazek, C. A., and Hicks, R. M., "Upper-Surface Modifications for $C_{\ell_{max}}$ Improvement of Selected NACA 6-Series Airfoils." NASA TM 78603, August 1979.

4. Bowden, Gensemer, and Skeen, "Engineering Summary of Airframe Icing Technical Data." FAA Technical Report ADS-4, December 1963.

Table 1 Airfoil Coordinates of Wing Section at Centerline of the IRT (WS 58) in Percent of the Chord.

Upper Surface		Lower Surface	
x	y	x	y
0	-.704	0	-.704
.015	-.250	.335	-1.474
.648	.791	.723	-1.858
1.138	2.372	1.216	-2.193
2.055	3.447	2.451	-2.760
3.953	4.941	4.926	-3.545
6.324	6.008	7.407	-4.130
9.486	6.735	14.223	-5.371
11.352	7.036	19.197	-5.395
13.439	7.502	24.175	-6.359
22.024	7.565	29.157	-6.658
24.996	7.581	34.142	-6.816
30.126	7.597	39.129	-6.870
34.783	7.534	44.122	-6.718
39.428	7.426	49.115	-6.449
44.409	7.110	54.111	-6.114
49.387	6.591	99.741	-2.794
54.360	5.891		
59.331	5.047		
62.111	4.526		
99.744	-2.606		

Table 2A Summary of Data from Icing Research Tunnel Runs, T = 25°F

Run	α degrees	V knots	LWC_3 gm/m	d microns	Specific Fluid Flow Rate ml /cm² min			Spray Time minutes	Time to Shed Center Panel minutes	Mode		Comments
					upper	lower	center			center	upper lower	
1	-.5	96	1.16	15	.0215	.0193	.0140	-	17:00+	NDI	AI	
2	1.2	96	1.16	15	.0201	.0198	.0140	-	6:30	NDI	AI	
3	7.8	96	1.16	15	.0232	.0170	.0113	-	8:00	NDI	AI	
4	12.5	96	1.16	15	.0170	.0170	.0140	-	8:45	NDI	AI	
5	-.5	96	1.50	15	.0272	.0198	.0091	-	5:00	NDI	AI	Shed in numerous pieces
6	1.2	96	1.50	15	.0226	.0198	.0113+	-	5:30	NDI	AI	
7	7.8	96	1.50	15	.0255	.0193	.0091	-	6:30	NDI	AI	
8	12.5	96	1.50	15	.0159	.0164	.0113	-	6:00	NDI	AI	
9	-.5	96	2.40	20	.0379	.0260	.0113	-	UND	NDI	AI	Ragged shedding
10	1.2	96	2.40	20	.0419	.0294	.0140+	-	6:30	NDI	AI	Partial shed at 3:00 min.
11	7.8	96	2.40	20	.0436	.0340	.0113	-	3:45	NDI	AI	
12	12.5	96	2.40	20	.0311	.0215	.0140	-	5:50	NDI	AI	Lower 50% shed at 2:45 min.
13	1.2	96	2.40	20	.040	.029	.026	2	10:20	De-ice	AI	
14	1.2	96	2.40	20	.0435	.0442	.0523	2	2:10	De-ice	AI	
15	1.2	96	2.40	20	.0435	.0442	.0141	2	80% 10:00+	De-ice	AI	Dissolved rather than shed
16A	1.2	96	2.40	20	.040	.029	.026	5	2:20	De-ice	AI	Temp. too high, 31°F in center,
16B	1.2	96	2.40	20	.036	.031	.026	5	13:10	De-ice	AI	repeat with correct temp. as run 16B
17	1.2	96	2.40	20	.040	.031	.026	5	5:36	De-ice	AI	Shed in pieces
18	1.2	96	2.40	20	NR	NR	.0786	10	4:20	De-ice	AI	80% shed at 2:37 min.
20	1.2	96	2.40	20	.040	.029	.052	10	14:10	De-ice	AI	60% shed at 4:00 min.
21	1.2	96	2.40	20	.040	.029	.106	10	2:50	De-ice	AI	
23	7.8	96	2.40	20	NR	NR	.052	2	2:05	De-ice	AI	Shed in small flakes

AI = Anti-ice
NDI = Natural De-ice

NR = Not Recorded
UND = Undefined

Table 2A Continued

Run	α degrees	V knots	LWC_3 gm/m	d microns	Specific Fluid Flow Rate ml/cm² min upper	lower	center	Spray Time minutes	Time to Shed Center Panel minutes	Mode center	upper lower	Comments
25	7.8	96	2.40	20	.040	.018	.026	5	6:43	De-ice	AI	
26	7.8	96	2.40	20	.040	.018	.052	5	6:43	De-ice	AI	
27	7.8	96	2.40	20	.039	.030	.0141	5	11:23	De-ice	AI	60% shed at 11:23 Remainder shed at α=18° after α change
29	7.8	96	2.40	20	.040	.029	.052	10	4:15	De-ice	AI	90% shed at 3:36 min.
40	-.5	175	.65	11	.025	.021	.024	-	6:00	NDI	AI	
41	1.2	175	.65	11	.024	.025	.019	-	9:04	NDI	AI	
42	7.8	175	.65	11	.022	.022	.017	-	7:42	NDI	AI	
43	12.0	175	.65	11	.022	.025	.017	-	7:15	NDI	AI	
44	-.5	175	.80	15	.054	.054	.026	-	UND	NDI	AI	No distinct bar, shed in pieces
45	1.2	175	.80	.5	.038	.035	.021	-	2:55	NDI	AI	
46	7.8	175	.80	15	.033	.031	.024	-	4:40	NDI	AI	30% shed at 2:30 min.
47	12.0	175	.80	15	.034	.029	.024	-	6:00	NDI	AI	
48	-.5	175	1.16	15	.064	.045	.033	-	NR	NDI	AI	
49	1.2	175	1.16	15	.054	.043	.033	-	NR	NDI	AI	
50	7.8	175	1.16	15	.050	.033	.026	-	7:48	NDI	AI	30% shed at 4:30 min.
51	12.0	175	1.16	15	.046	.031	.028	-	3:00	NDI	AI	
52	1.2	175	1.16	15	NR	NR	.026	3:00	9:40	De-ice	AI	
53	1.2	175	1.16	15	.057	.043	.052	3:00	5:00	De-ice	AI	90% shed at 5:00 min.
54	1.2	175	1.16	15	NR	NR	.079	3:00	3:28	De-ice	AI	
55	1.2	175	1.16	15	NR	NR	.026	6:00	17:30	De-ice	AI	Shed with α changed to 2.2°
56	1.2	175	1.16	15	NR	NR	.052	6:00	8:53	De-ice	AI	
57	1.2	175	1.16	15	NR	NR	.079	6:00	8:50	De-ice	AI	
62	7.8	175	1.16	15	NR	NR	.052	3:00	3:04	De-ice	AI	
64	7.8	175	1.16	15	NR	NR	.026	6:00	11:18	De-ice	AI	
65	7.8	175	1.16	15	NR	NR	.052	6:00	5:37	De-ice	AI	
65-0	7.8	175	1.16	15	NR	NR	.052	6:00	4:56	De-ice	AI	De-iced with ± .5° pitch oscillation
66	7.8	175	1.16	15	NR	NR	.079	6:00	3:13	De-ice	AI	
68	7.8	175	1.16	15	NR	NR	.052	10:00	4:44	De-ice	AI	

Table 2B Summary of Data from Icing Research Tunnel Runs, T = 5°F

Run	α degrees	V knots	LWC gm/m³	d microns	Specific Fluid Flow Rate ml/cm² min upper	lower	center	Spray Time minutes	Time to Shed Center Panel minutes	Mode center	upper lower	Comments
79	-.5	96	1.16	15								
80	1.2	96	1.16	15	.042	.033	.014	-	NR	NDI	AI	
81	7.8	96	1.16	15	.056	.033	.014	-	2:50	NDI	AI	
82	12.0	96	1.16	15	.026	.035	.009	-	2:10	NDI	AI	
83	-.5	96	1.50	15	.042	.045	.019	-	9:15	NDI	AI	
84	1.2	96	1.50	15	.040	.039	.009	-	4:23	NDI	AI	First shed at 1:40 min@, thick = .05"
85	7.8	96	1.50	15	.038	.035	.009	-	7:17	NDI	AI	First shed at 2:53 min. at thick = .035"
86	12.0	96	1.50	15	.038	.035	.012	-	4:15	NDI	AI	
87	-.5	96	2.40	20	.071	.085	.043	-	7:30+	NDI	AI	Did not shed until α changed to 1.0°
92	1.2	96	2.40	20	.097	.097	.052	2	13:40+	De-ice	AI	
95	1.2	96	2.40	20	.077	.056	.052	5	15:23+	De-ice	AI	α changed to 1.8° for total shed
98	1.2	96	2.40	20	.137	.118	.052	10	13:00+	De-ice	AI	α changed to 2.0° for shed
101	7.8	96	2.40	20	.137	.129	.052	2	6:01	De-ice	AI	
103	7.8	96	2.40	20	.137	.108	.038	5	5:04	De-ice	AI	
104	7.8	96	2.40	20	.137	.129	.052	5	3:01	De-ice	AI	
105	7.8	96	2.40	20	.036	.022	.079	5	1:09	De-ice	AI	Natural de-ice threshold on lower panel
107	7.8	96	2.40	20	.137	.129	.052	10	1:48	De-ice	AI	
113	12.0	96	2.40	20	.117	.087	.052	5	8:18	De-ice	AI	
118	-.5	175	.65	11	.079	.077	.043	-	8:40	NDI	AI	
119	1.2	175	.65	11	.075	.066	.017	-	UND	NDI	AI	Fairly continuous shedding like anti-ice
120	7.8	175	.65	11	.075	.060	.009	-	1:33	NDI	AI	Second total shed at 3:50

AI = Anti-ice
NDI = Natural De-ice
NR = Not Recorded
UND = Undefined

Table 2B Continued

Run	α degrees	V knots	LWC_3 gm/m	d microns	Specific Fluid Flow Rate ml/cm^2 min upper	lower	center	Spray Time minutes	Time to Shed Center Panel minutes	Mode center	upper lower	Comments
119B	1.7	175	.65	11	.194	.162	.043	-	NR	NDI	AI	Flow values increased over 119, no significant changes in performance
120B	7.8	175	.65	11	.194	.162	.043	-	NR	NDI	AI	Center value = anti-ice, compare to run 120, no significant change
121	12.0	175	.65	11	.032	.037	.012	-	1:48	NDI	AI	60% shed
123	1.2	175	.80	15	NR	NR	NR	-	NR	NDI	AI	Premature termination, tunnel malfunction
124	7.8	175	.80	15	.075	.070	.012	-	1:20	NDI	AI	
125	12.0	175	.80	15	.071	.068	.017	-	2:28	NDI	AI	Shed in slushy pieces
126	-.5	175	1.16	15	.056	.067	.038	-	4:30	NDI	AI	
127	1.2	175	1.16	15	.056	.062	.026	-	UND	NDI	AI	
128	7.8	175	1.16	15	.033	.054	.019	-	UND	NDI	AI	
129	12.0	175	1.16	15	.045	.056	.043	-	UND	NDI	AI	Difficult to establish threshold values
134	1.2	175	1.16	15	NR	NR	.052	6	4:10	De-ice	AI	
135	1.2	175	1.16	15	NR	NR	.079	6	1:25	De-ice	AI	
139	7.8	175	1.16	15	NR	NR	.026	3	3:45	De-ice	AI	
140	7.8	175	1.16	15	NR	NR	.052	3	1:41	De-ice	AI	
141	7.8	175	1.16	15	NR	NR	.014	3	10:52	De-ice	AI	
142	7.8	175	1.16	15	NR	NR	.026	6	1:45	De-ice	AI	
143	7.8	175	1.16	15	NR	NR	.052	6	1:40	De-ice	AI	
144	7.8	175	1.16	15	NR	NR	.014	6	1:12	De-ice	AI	

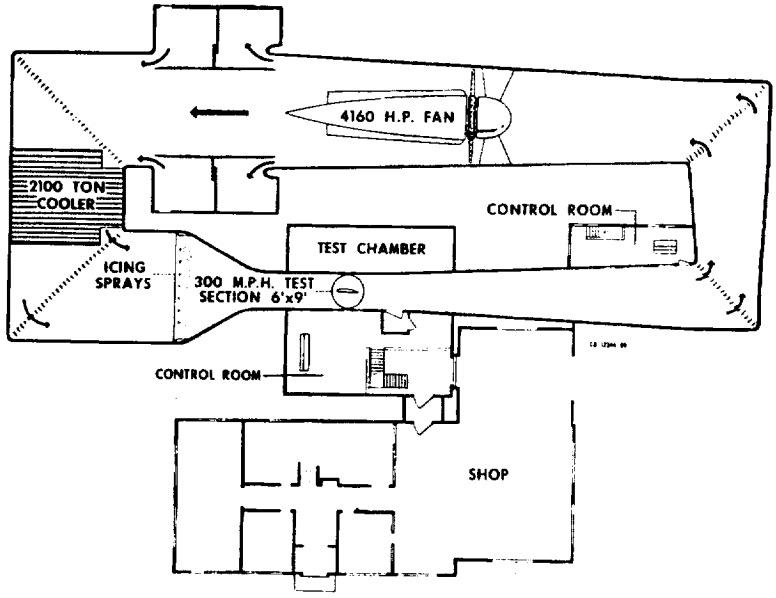

Figure 1. - NASA Lewis Icing Research Tunnel.

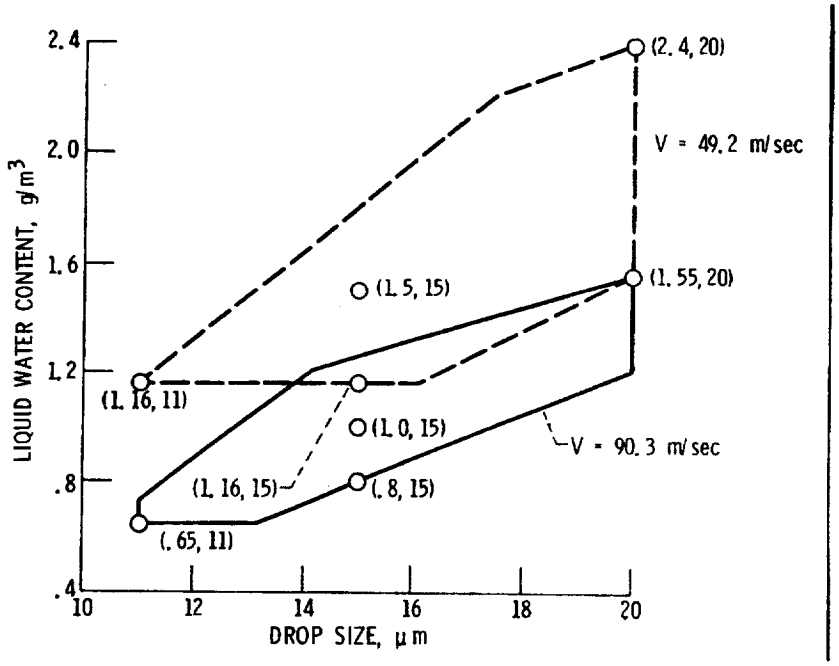

Figure 2. - IRT Operating Envelopes and Test Points.

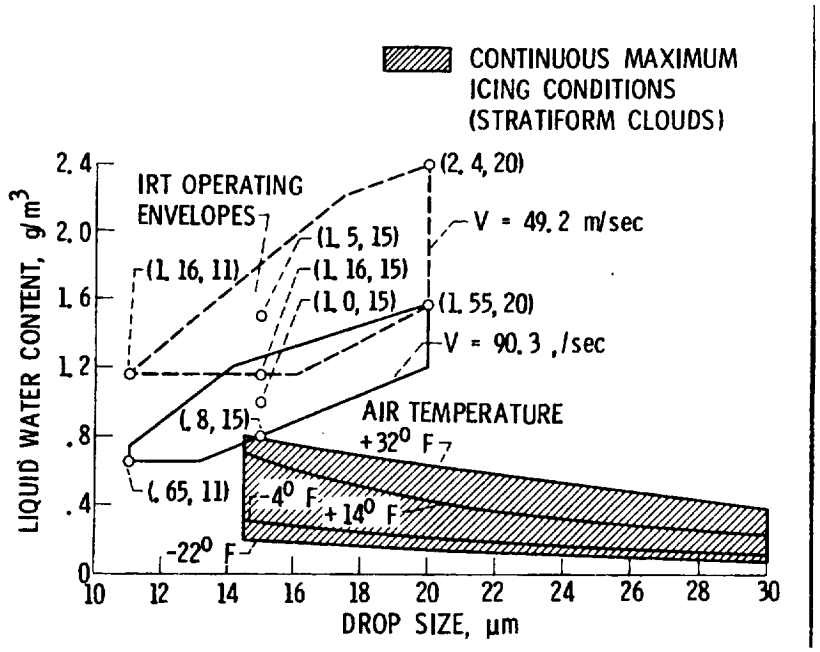

Figure 3. - Continuous Maximum Icing Conditions (ref. 1) and IRT operating envelopes.

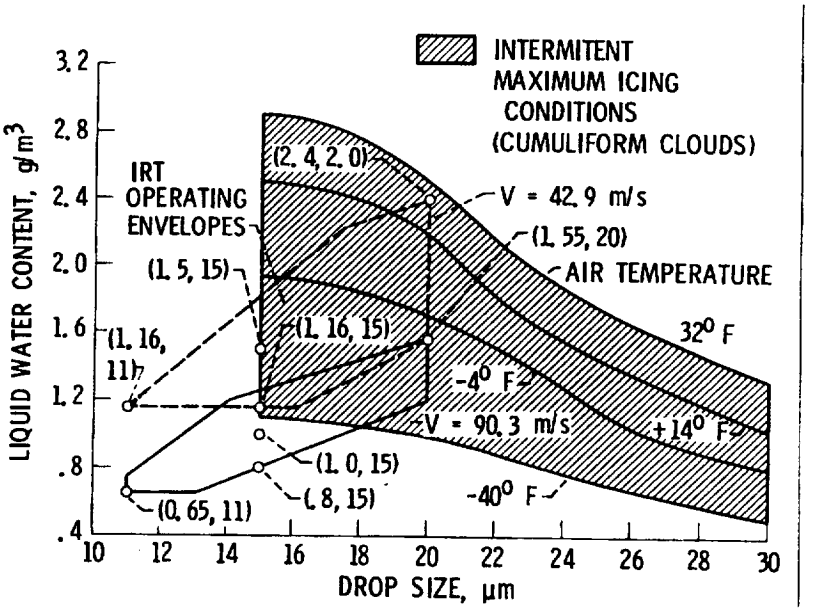

Figure 4. - Intermittent Maximum Icing Conditions (ref. 1) and operating envelopes.

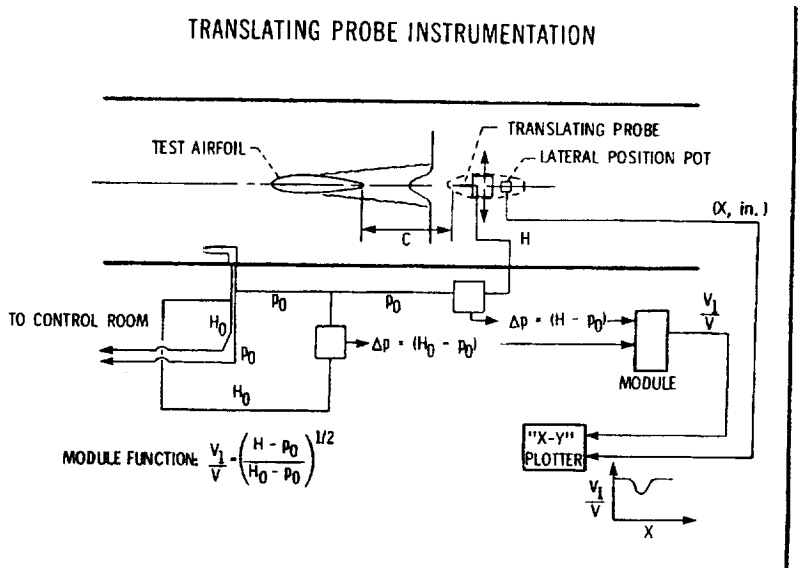

Figure 5. - Schematic of Wake-Survey Probe Instrumentation.

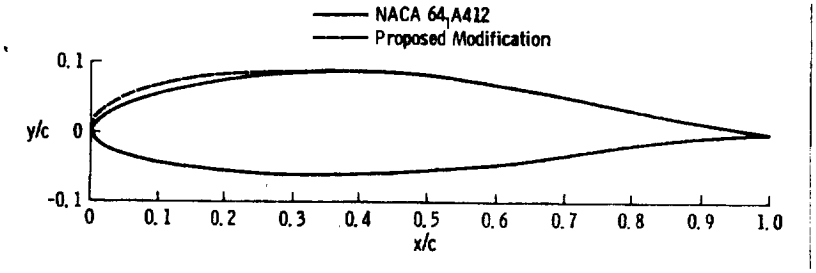

Figure 6. - Hicks Modification on a NACA 64_1A412 Airfoil.

Figure 7. - Wing Section Installed in the NASA Lewis Icing Research Tunnel.

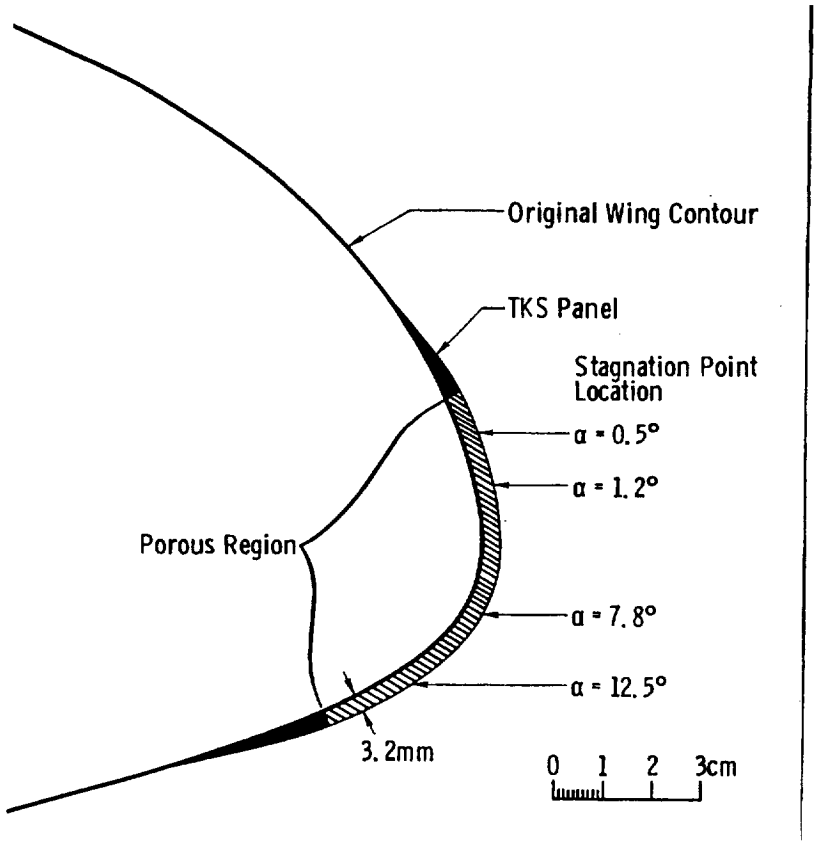

Figure 8. - Cross Section of the T.K.S. Porous Panel Installed on the Test Wing at WS 58.

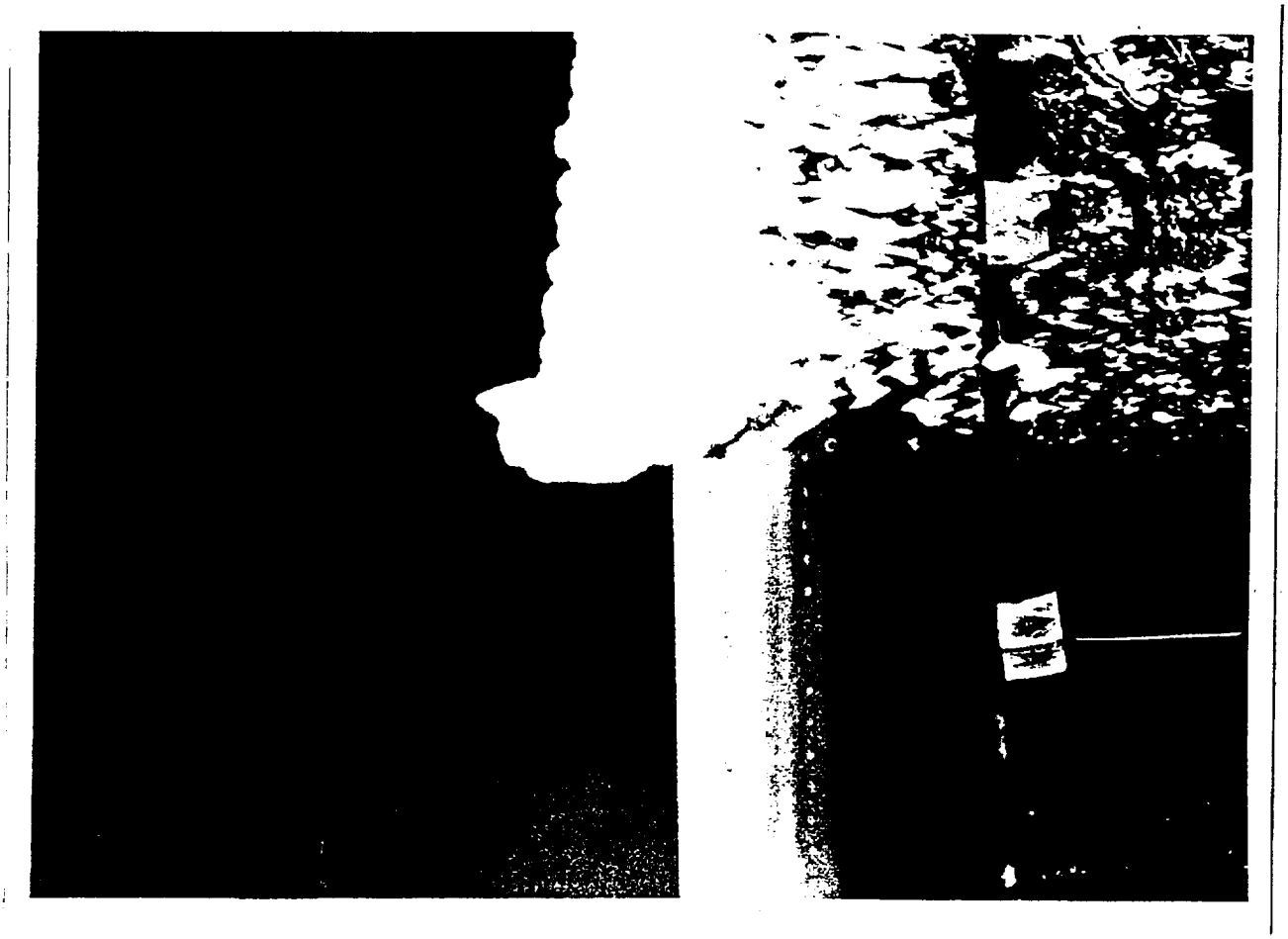

Figure 9. - Porous Panel Installed on the Wing.

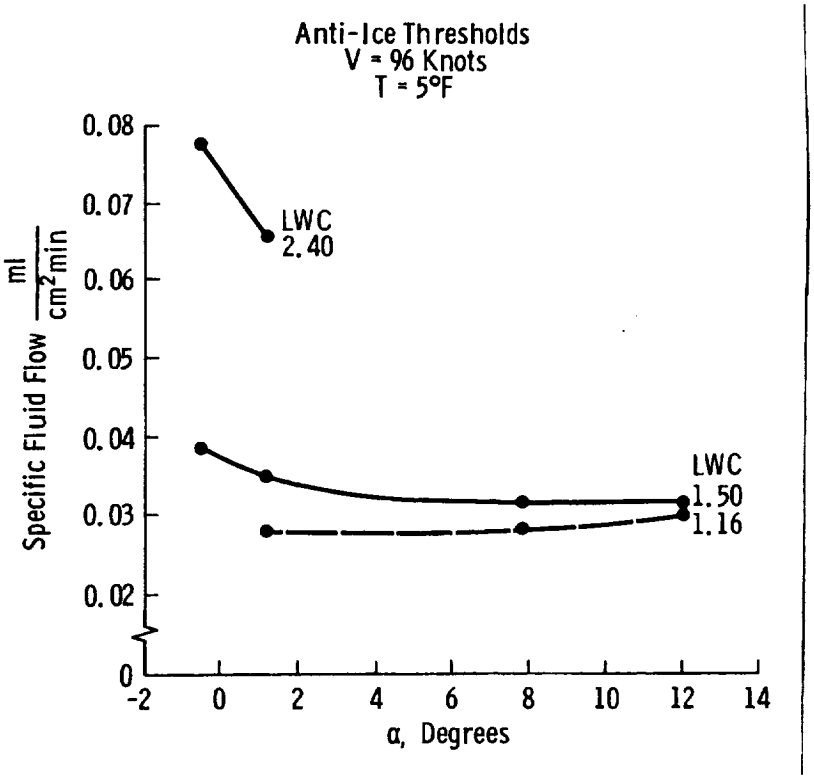

(a)

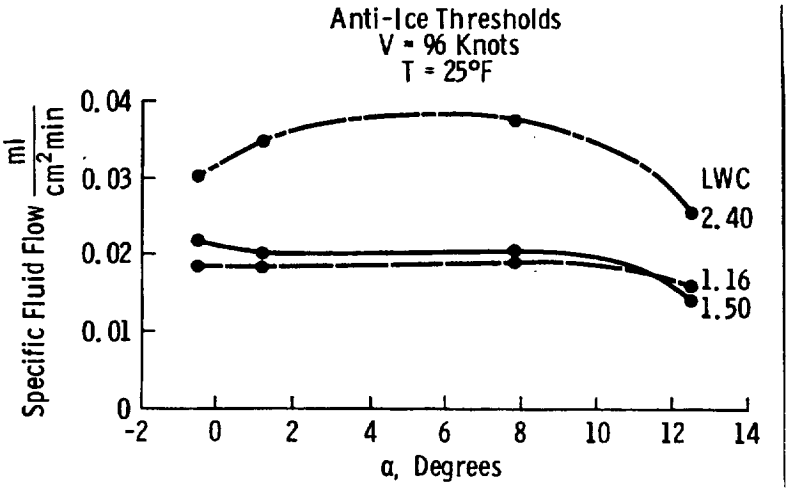

(b)

Figure 10. - Minimum Glycol Flow Rates Required to Maintain Anti-Icing.

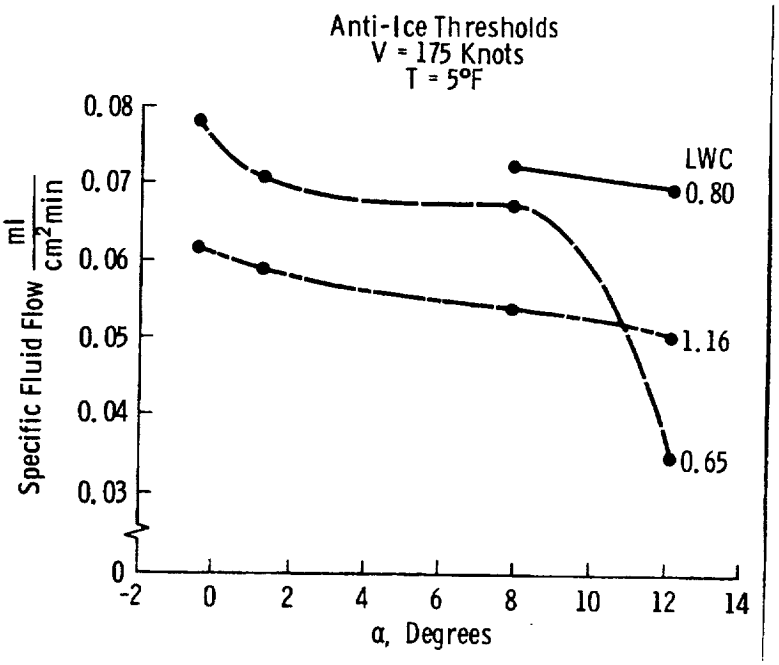

(c)

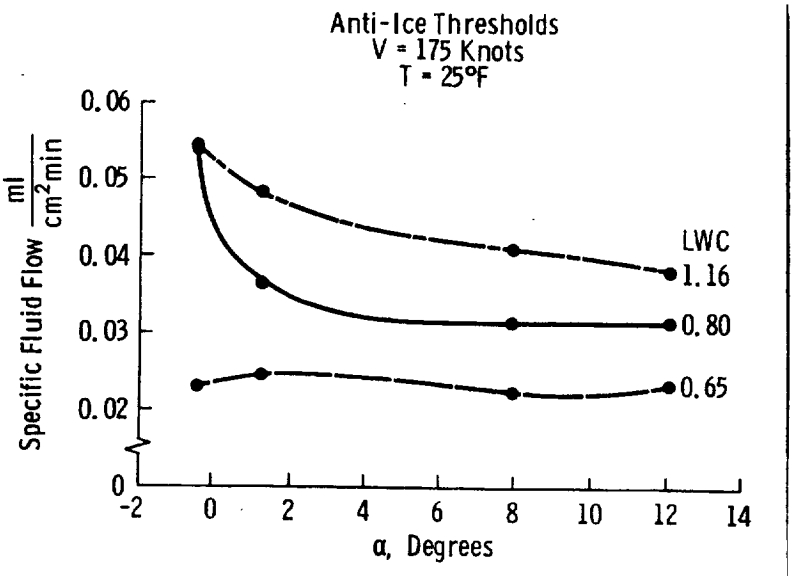

(d)

Figure 10. - (Continued.)

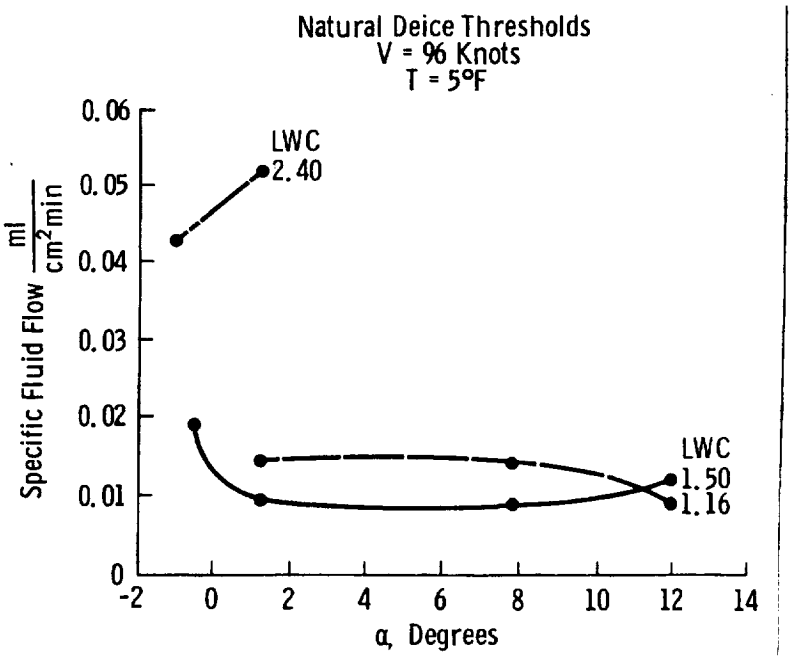

(a)

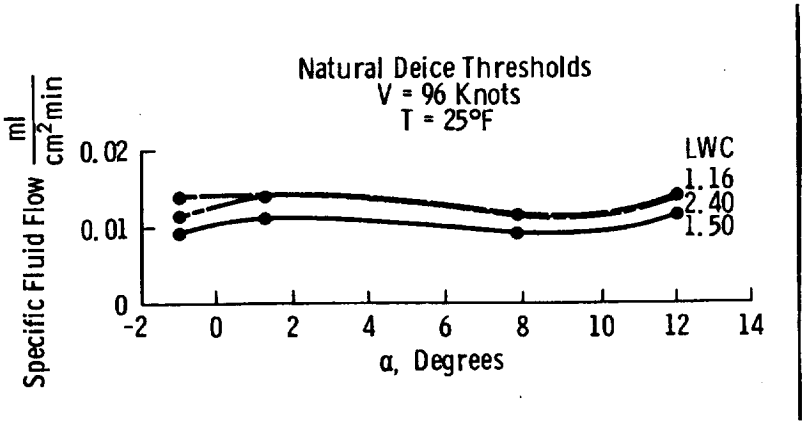

(b)

Figure 11. - Minimum Glycol Flow Rates Required to Maintain Natural Deicing.

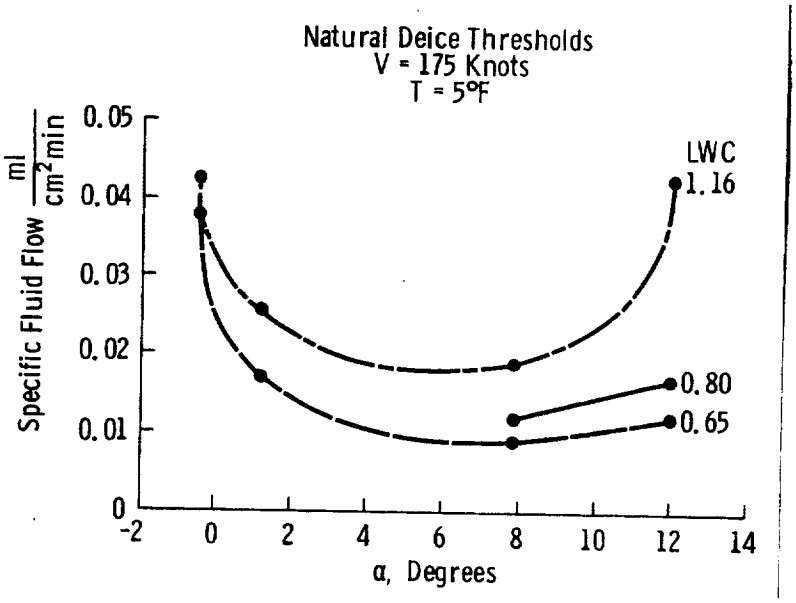

(c)

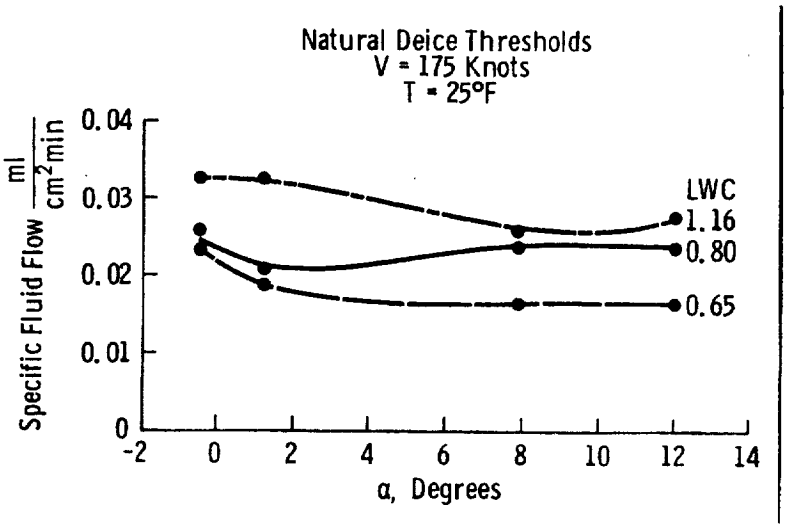

(d)

Figure 11. - (Continued.)

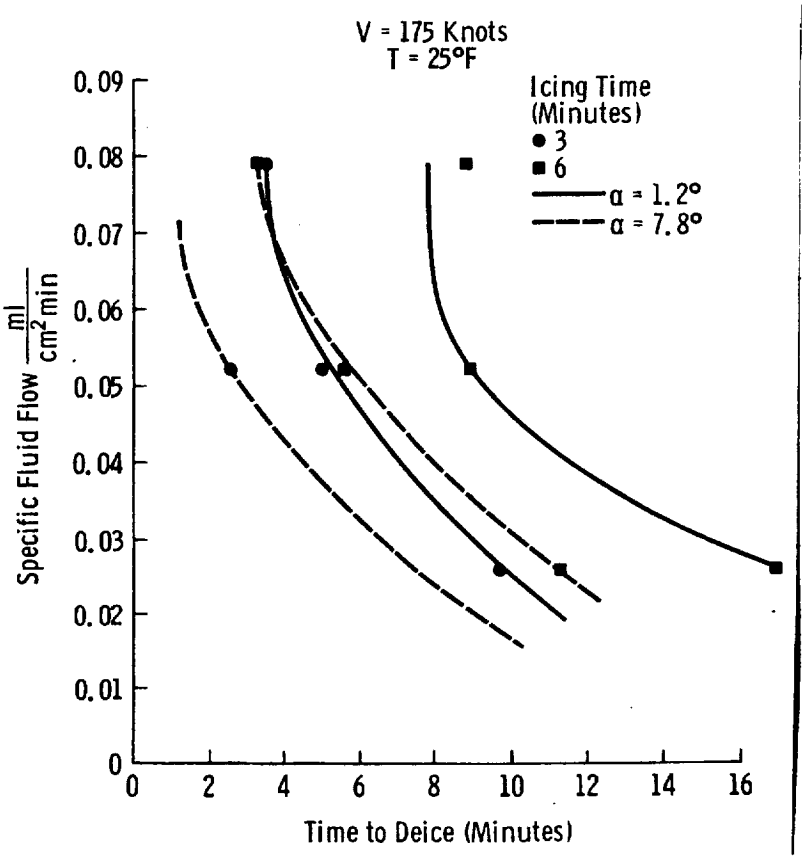

Figure 12. - Effect of Angle of Attack and Glycol Flow Rate on Time to Deice.

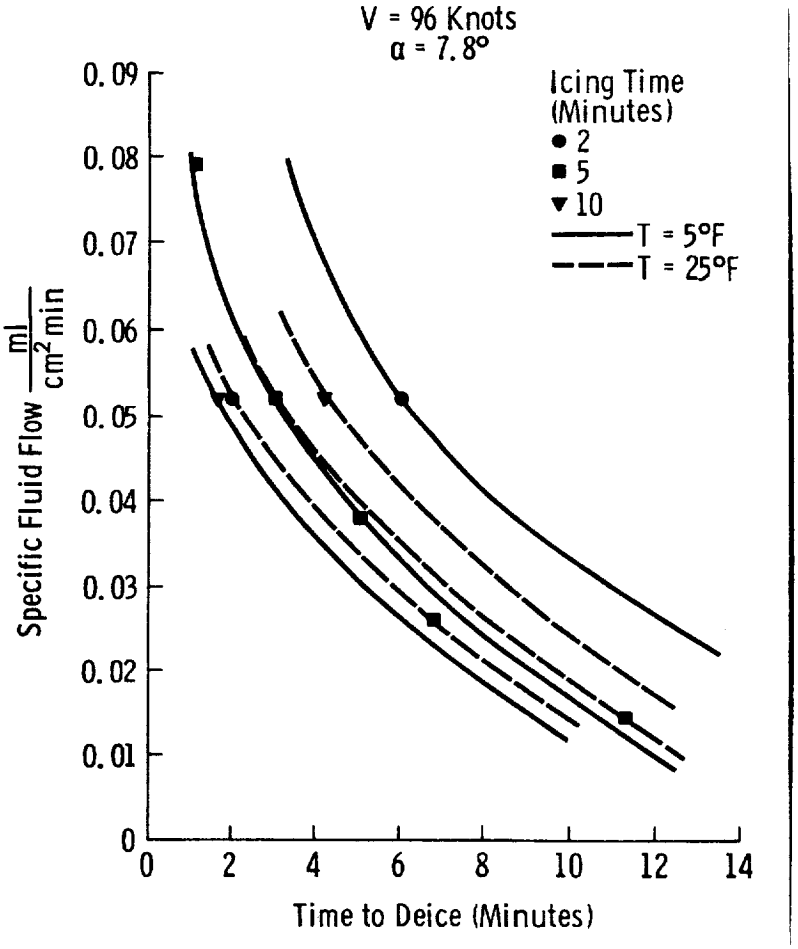

Figure 13. - Effect of Temperature and Glycol Flow Rate on Time to Deice.

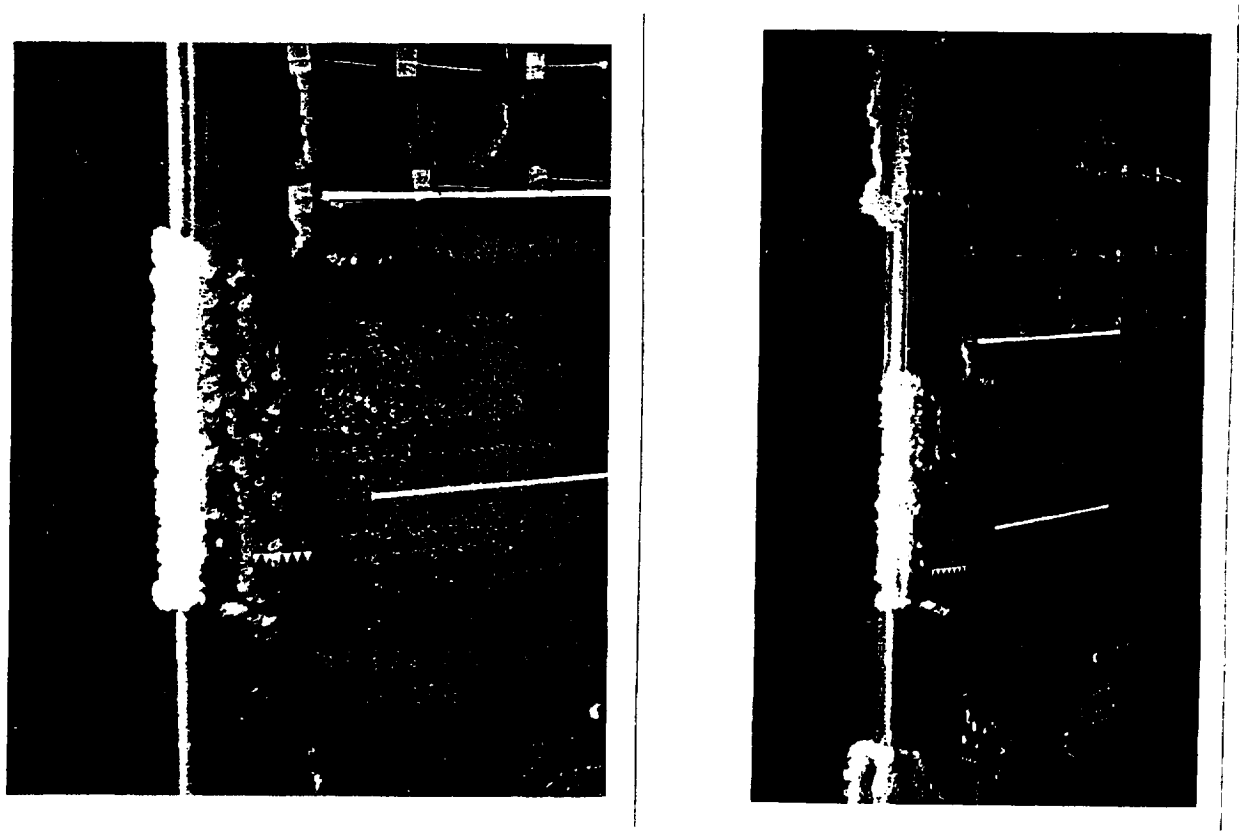

(a) 0 min (b) 2 min

Figure 14. - Deicing Time Sequence for Ice Cap Formed by 10 min Exposure with LWC = 2.4 gm/m^3, V = 96 knots, α = 7.8°, T = 25°F. Specific Fluid Flow = 0.052 ml/cm^2/min.

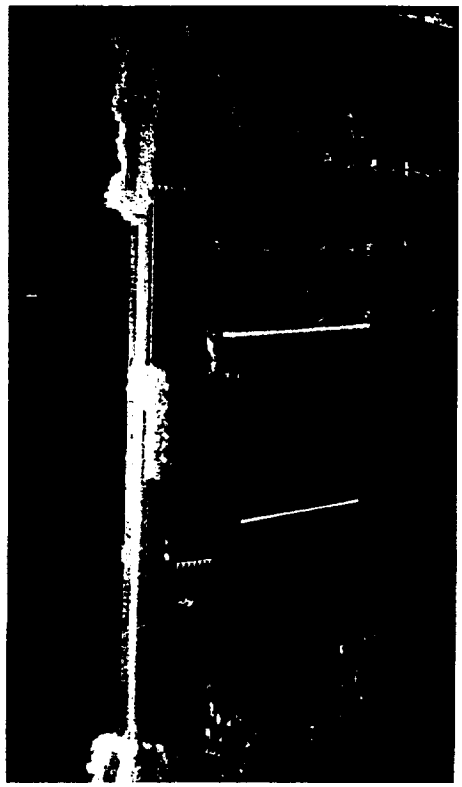

(c) 3 min

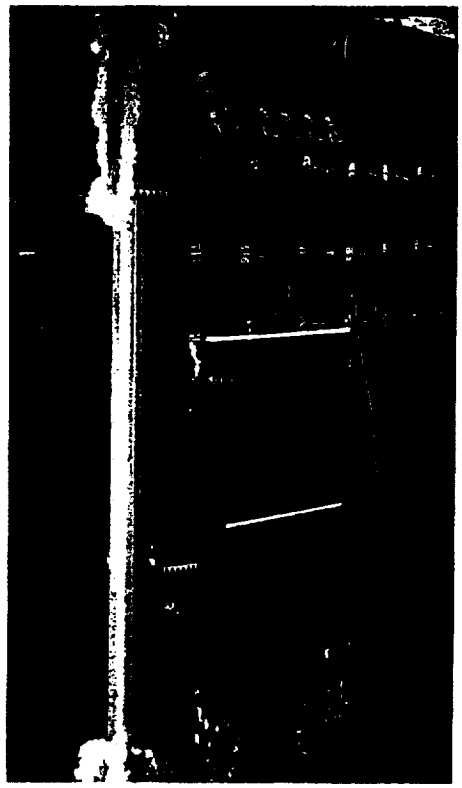

(d) 4 min

Figure 14. - (Continued.)

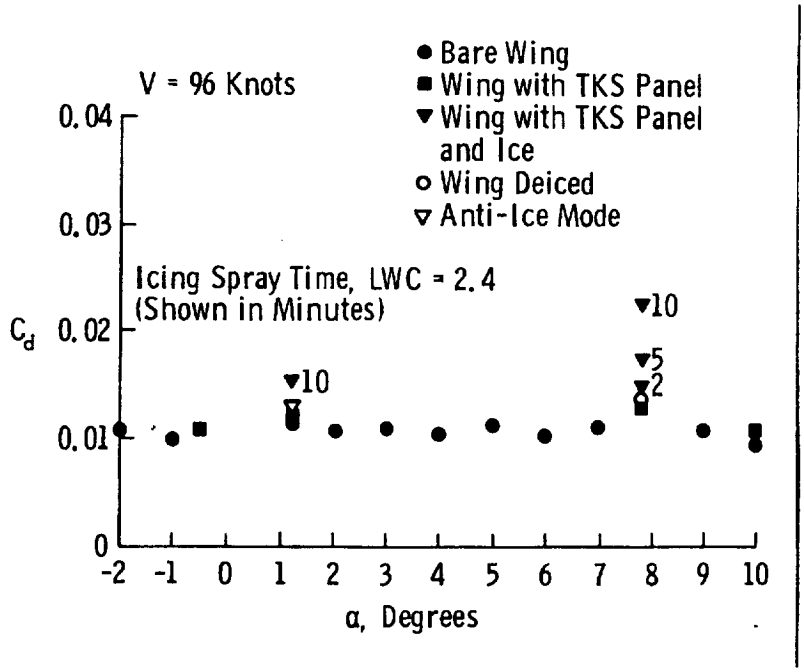

Figure 15. - Effect of Icing System on Various Amounts of Ice on Section Drag Coefficient.